Novel chemically amplified resists incorporating anionic photoacid generator functional groups for sub-50-nm half-pitch lithography

Kenneth E. Gonsalves,*[a] Mingxing Wang,[a] Cheng-Tsung Lee,[b] Wang Yueh,[c] Melina Tapia-Tapia,[d] Nikola Batina[d] and Clifford L. Henderson[b]

Received 21st October 2008, Accepted 9th February 2009
First published as an Advance Article on the web 9th March 2009
DOI: 10.1039/b818612j

A series of chemically amplified resists based on polymers of 4-hydroxystyrene, 2-ethyl-2-adamantyl methacrylate and a monomer-bound anionic photoacid generator (PAG) were prepared and characterized. Specifically, the following PAGs were separately incorporated into the main-chain of the polymers: the isomers triphenylsulfonium salt 2-(methacryloxy)-4-trifluoromethyl benzenesulfonate and triphenylsulfonium salt 4-(methacryloxy)-2-trifluoromethyl benzenesulfonate (CF3 PAG); triphenylsulfonium salt 4-(methacryloxy)-3-nitro-benzenesulfonate (NO2 PAG); and triphenylsulfonium salt of 1,1,2-trifluorobutanesulfonate methacrylate (MTFB PAG). Triphenylsulfonium salt 4-(methacryloxy)-2,3,5,6-tetrafluorobenzenesulfonate (F4 PAG) was used as the reference PAG. The intrinsic lithography performance of these polymer-bound PAG resists showed sub-50-nm half-pitch resolution and <5 nm LER (3σ) under 100 keV electron beam patterning. The relative sensitivity of these materials under 100 keV e-beam exposure was MTFB PAG ≥ F4 PAG > CF3 PAG > NO2 PAG. Resolved pattern sizes of 40 and 32.5 nm half-pitch were obtained for fluorinated PAGs (such as MTFB PAG and F4 PAG) bound polymer resists under EUV interference lithography. The surface roughness was inspected with AFM.

1. Introduction

The microelectronic industry has made remarkable progress with the development of integrated circuit (IC) technology, which depends on the fabrication of smaller feature sizes. On one hand, extreme ultraviolet (EUV) has emerged as the promising candidate to meet the resolution requirements of the microelectronic industry roadmap.[1–3] On the other hand, to develop novel photoresist materials with the required critical imaging properties (such as high resolution, high sensitivity, and lower line-edge roughness) is simultaneously indispensable and one of the most challenging issues for next-generation lithography technology. In the chemically amplified resist (CAR) system, the photoacid generators (PAGs) are key materials in the curing and imaging processes of photosensitive polymeric materials.[4,5] The conventional CAR formulations are complex mixtures of a protected polymer matrix and a small molecule PAG. These kind of PAG blend CAR materials have inherent incompatibility that can lead to PAG phase separation, non-uniform initial PAG and photoacid distribution, as well as acid migration during the post-exposure baking (PEB) processes. These problems result in the tradeoff between achieving the desired characteristics of high resolution, high sensitivity, and low line-edge roughness.[6] To alleviate these problems, some new fluorinated blend PAGs that provide strong acid, good lithographic performance, and process compatibility have been developed.[7–9] Molecular resists, also show promise for E-beam and EUV lithography.[10–17] Several systems with ionic or non-ionic PAG grafting into the main-chain of polymer have been recently reported.[18–25] We have reported that anionic PAGs incorporated into the main chain of the 4-hydroxystyrene and 2-ethyl-2-adamantyl methacrylate-based polymers showed improved lithographic performance, such as high PAG loading, relatively faster photospeed, higher stability, lower outgassing, and lower line edge roughness (LER) than the corresponding cationic PAG bound polymer or PAG blend polymer resists.[21–23,25–26] The higher PAG loading through anionic binding of PAG onto the polymer resin of a resist material results in higher density however smaller deprotection volume created by each acid molecule, that leads to reduced image blur and a smoother deprotection front without losing the photospeed of the resist material.[27] Herein we report a series of PAG-bound polymer photoresists based on anionic vinyl monomer PAGs with strong electronic-withdrawing groups, and hydroxystrene (HOST) and 2-ethyl-2-adamantyl-methacrylate (EAMA) with moderate molecular weight and controlled PAG mol percent (Fig. 1 and 2). Fig. 2 also outlines the anticipated advantages of polymer resist microstructures incorporating PAGs in the resist backbone. An investigation of their preparation, characterization, thermostability, acid-generating efficiency, absorbance and intrinsic lithographic performance under E-beam and initial exposure EUV are also outlined.

[a]*Polymer Nanotechnology Laboratory at Center for Optoelectronic and Optical Communications, Department of Chemistry, University of North Carolina, Charlotte, North Carolina, 28223, USA*
[b]*School of Chemical & Biomolecular Engineering, Georgia Institute of Technology, AtlantaGeorgia, 30332, USA*
[c]*Intel Corp., Hillsboro, OR, 97124, USA*
[d]*Lab. de Nanotecnologia e Ingenieria Molecular, Area de Electroquimica, Depto. de Quimica, CBI, Universidad Autonoma Metropolitana–Iztapalapa, Delegacion Iztapalapa, Av. San Rafael Atlixco No. 186, Col. Vicentina C.P., 09340 Mexico, DF, Mexico. E-mail: kegonsal@uncc.edu; Fax: +1 (01)704 687 8241*

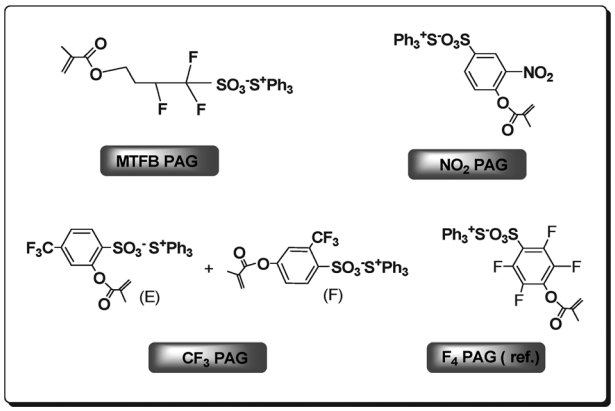

Fig. 1 Photoacid generator (PAG) structures.

2. Experimental

Materials

2,2′-Azobisisobutyronitrile (AIBN) and propylene glycol-1-monomethyl ether 2-acetate (PGMEA) and triflic acid were purchased from Sigma Aldrich. 1,1,1,3,3,3-Hexamethyl disilazane (HMDS) was from ICN Biomedicals, Inc. 2-Ethyl-2-adamantyl-methacrylate (EAMA) and 2.38 wt% tetramethylammonium hydroxide (TMAH) were supplied by AZ Electronic Materials Ltd. Hydroxystrene (HOST) was prepared by the hydrolysis of 4-acetoxystyrene purchased from TCI America. Tetrahydrofuran (THF) and acetonitrile were dried (over sodium, calcium hydride) before use. Photoacid generators (PAGs) were reported previously.[25–29] All chemicals and solvents were used without further purification unless otherwise noted.

Analytical measurement

The NMR was performed on a JEOL500 spectrometer with DMSO-d_6 or $CDCl_3$ and TMS as the solvent and internal standard, respectively. UV-VIS absorption spectra were obtained on a HP 8453 UV-Visible spectrophotometer. Gel permeation chromatography (GPC, Waters Breeze software) was performed with THF as the eluent. The molecular weights of polymers were calculated with respect to polystyrene as narrow M_w standards. Thermal analysis was performed on a TA instrument, Hi-Res TGA 2950 Thermogravimetric Analyzer 7, and differential scanning calorimetry (DSC 2920) under a nitrogen atmosphere at a heating rate of 10 °C min^{-1}. TGA was used to determine the decomposition temperature (T_d, at 3% weight loss).

Synthesis of polymers

Polymers were prepared by free radical polymerization in sealed pressure vessels (Scheme 1). Monomers HOST, EAMA, anionic PAGs, and AIBN as a free radical initiator (5 mole % to the monomers) were dissolved in freshly distilled anhydrous THF and acetonitrile (v/v = 1 : 1). Polymerization was performed at 65 °C for 24 hours. The polymer solutions were precipitated into a large amount of diethyl ether or petroleum ether and dried. The crude products were then redissolved in THF and precipitated with petroleum ether twice, and then dried in vacuum for 24 hours. The polymer composition was calculated by ^{1}H NMR. The results are given in Table 1.

Resist processing

Resist film optical absorption. Resist solutions (5 wt%) were prepared by dissolving the solid polymer powders into cyclohexanone and filtering the resulting solutions through 0.2 μm syringe filters. Resist films for optical absorption measurements were prepared by spin-coating the resist solution onto fused silica discs (20 mm in diameter and 2 mm in thickness, Edmund Optics Inc.) followed by a post-apply baking (PAB) at 100 °C for 90 s.

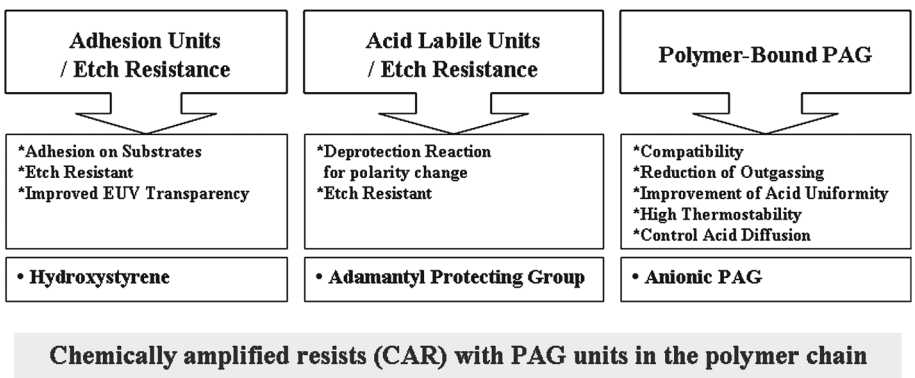

Fig. 2 Design of polymer microstructures for EUV lithography.

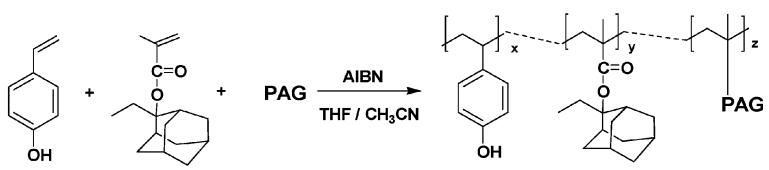

Scheme 1 Synthetic scheme of polymers

Table 1 Polymerization and characterization results

Polymer (resist)	Mole feed mole ratio			Polymer composition (mol%)			Yield [b] (wt%)	M_w (PDI)	T_d [c]/°C	T_g [d]/°C
	HOST	EAMA	PAG	HOST	EAMA	PAG				
HE-F4 PAG [a]	25	72.5	2.5	35.0	57.9	7.1	37.3	3600 (1.6)	145	NA
HE-CF3 PAG	35	60	5.0	40.3	51.4	8.3	31.3	3700 (2.0)	159	NA
HE-NO2 PAG	35	60	5.0	37.8	54.6	7.6	36.2	3900 (2.1)	162	NA
HE-MTFB PAG	30	65	5.0	38.5	56.2	5.3	42.3	2600 (1.6)	170	117
HE-MTFB PAG[e]	30	63.0	7.0	38.3	53.6	8.1	39.2	3100 (1.9)	173	131

[a] See ref. 21, 25; HE stands for HOST-EAMA. PAG abbreviations as in Fig 1 above. [b] Weight percentage relative to the initial reactant feed. [c] The decomposition temperature was determined according to weight loss below 3.0%. [d] Could not be determined by DSC. [e] a and e: EUV samples.

The resist film absorption in the deep ultraviolet (DUV) wavelength region (190–370 nm) was collected.

Resist photospeed, contrast, and resolution under electron-beam radiation and EUV. For the photospeed and resist contrast tests under electron-beam (e-beam) radiation, a bare silicon wafer was first primed with a solution containing 20 wt% HMDS and 80 wt% PGMEA. Each resist film was prepared by spin-coating the resist solution onto the primed wafer and PAB the resulting film at 100 °C for 90 s. The resulting film thickness values were approximately 135 nm measured by a variable-angle spectroscopic ellipsometer (V-VASE, J. A. Woollam). For intrinsic resolution tests of each resist, the same process for resist film preparation was applied but a wafer containing free-standing low-stress silicon nitride membrane windows was fabricated and used as the substrate. Imaging of the resist over these nitride windows helps eliminate the effect of electron backscattering from the substrate, thus producing a very high aerial image contrast in the e-beam for patterning which closely approximates a digital aerial image.[26] The resist film thicknesses on these nitride window substrates was approximately 70 nm. Resist film thicknesses were measured also using a variable-angle spectroscopic ellipsometer (V-VASE, J. A. Woollam). Resist films were subsequently patterned using a JEOL JBX-9300FS e-beam lithography system with a 100 keV acceleration voltage. The electron-beam current was set as 2 nA and the single-pixel beam-diameter was 8 nm. The resist film was post-exposure baked (PEB) at 100 °C for 90 s and developed in conventional 2.38 wt% TMAH for 15 s and rinsed with deionized water. For the determination of resist photospeed and contrast under EB, a profilometer (Model number P-15, KLA-Tencor Corp.) was used to measure the film thickness after development in a series of large square exposed areas subjected to different e-beam radiation doses after development. After development the film thickness data was used to produce a conventional contrast curve for each resist. The photospeed was determined as the dose which results in 50% film thickness loss. For the determination of resist resolution, the backside of the silicon nitride membrane was sputtered with 20 nm of gold to act as an anti-charging layer for scanning electron microscope (SEM) imaging. The pattern was imaged in a top-down mode using a LEO 1530 thermally assisted field emission SEM with a 3 kV acceleration voltage and a 50 000× magnification. The edge roughness was determined by an off-line SEM image analysis, and the whole-spatial frequency LER (3σ) was determined by averaging over 5 individual 50 nm wide lines with 1 μm inspection length. The EUV exposures were carried out using the Swiss light source beamline at Paul Scherrer Institute, Villingen, Switzerland. The exposure condition was same as e-beam exposure except for the film thickness of approximately 120 nm.

3. Results and discussion

The polymers were prepared by free radical polymerization with yields from 31.3–42.3%. The PAG contents ranged between 7.1, 8.3, 7.6 and 5.3 or 8.1% (mole ratio) for HOST-EAMA-F4 PAG(HE-F4 PAG), HOST-EAMA-CF3 PAG (HE-CF3 PAG), HOST-EAMA-NO2 PAG (HE-NO2 PAG), and HOST-EAMA-MTFB PAG (HE-MTFB PAG), respectively. The molar composition of each unit in the polymers was determined by ^{1}H NMR. The characteristic peaks: around 9.1 ppm is assigned to the proton of hydroxyl group of HOST, 7.6–7.8 ppm is assigned to the protons from PAG's cation TPS, 6.6–7.1 ppm from HOST and PAG's anionic part, 0.7–2.6 ppm from the EAMA and main-chain of polymer. The molar composition was calculated based on the integration ratios of the above corresponding peak. The results of the molecular weights showed the polymer HE-CF3 PAG, HE-NO2 PAG had M_w of 3700 with PDI 2.0 and 3900 with PDI 2.1, compared with HE-F4 PAG of M_w of 3600 with PDI 1.6. The polymer HE-MTFB PAG had a lower M_w 2600 with PDI 1.6, which showed that the MTFB PAG is not as active as CF3, NO2 and F4 PAG aromatic structures. The thermal stability of the polymers was identified by estimating the percentage of the weight loss of the polymer on thermal decomposition using TGA. The polymer HE-MTFB PAG (T_d 170 °C) is superior to HE-CF3 PAG, HE-NO2 PAG and HE-F4 PAG (T_d: 159, 162 and 145 °C, respectively). It was found that the polymer bound PAG resist showed less weight loss (3.69%, 4.22%, 4.17%) for HE-MTFB PAG, HE-CF3 PAG, HE-NO2 PAG, respectively than the polymer HE-F4 PAG (8.99%) at 170 °C. The glass transition temperature of polymer HE-MTFB PAG was 117 °C, the other polymers showed no obvious T_g. Based on comparisons of the polymer structures, this suggests that the incorporation of the fluorinated alkyl chain moiety in the HE-MTFB PAG unit provides some additional flexibility or mobility to the polymer chain that allows for a glass transition at temperatures lower than the polymer decomposition temperatures. The other polymers appear to be relatively rigid, likely resulting from the restrictions to motion provided by the bulky aromatic PAG structures.[25]

The results of the acid generation experiments showed that the acid yield (*i.e.* the moles of photoacid produced per mole of photoacid generator in the polymer) for HE-MTFB PAG,

HE-NO2 PAG, HE-F4 PAG, HE-CF3 PAG are 0.81, 0.74, 0.68, and 0.54 at a dose of 150 mJ cm^{-2} under DUV, respectively.[29]

The DUV (220–280 nm) absorption of the various resist materials are shown in Fig. 3 and the film absorbances at 254 nm wavelength were found to be in the following order: HE-CF3 PAG (2.02 μm^{-1}) > HE-NO2 PAG (1.29 μm^{-1}) > HE-MTFB PAG (0.71 μm^{-1}) >HE-F4 PAG (0.53 μm^{-1}). Since all these polymers have a similar HOST ratio and the HOST monomer has a substantially lower absorbance in general than that of the PAG monomers (*i.e.* typically HOST monomer molar absorptivity is on the order of 10% of the PAG monomers), and given that the EAMA unit does not contribute to any significant absorption at the DUV wavelength, the overall absorption differences among these resist polymers can be mainly ascribed to differences between the various PAG molar absorptivities and their loadings.[30] Strong absorption results in poor resist profiles, whereas low absorption leads to poor resist sensitivity. These acid generation and resist absorbance studies indicate that the MTFB PAG, NO2 PAG, and the F4 PAGs all are promising candidates for polymer-bound anionic PAGs for optical lithography applications.

Resist contrast results under e-beam radiation are illustrated in Fig. 4. The photospeed of the resists when using 100 keV e-beam exposure was found to be 24.0, 24.0, 59.0 and 108.0 $\mu C\ cm^{-2}$ for the HE-MTFB PAG, HE-F4 PAG, HE-CF3 PAG, and HE-NO2 PAG resists, respectively. Consistent with the optical results, the HE-MTFB PAG was observed to produce the fastest photospeed even though it contains a lower PAG loading (5.3 mol%) than the other resists. However, unlike the optical case, the sensitivity of the F4 and MTFB PAGs materials was virtually the same. The SEM images of the polymer-bound PAG resists

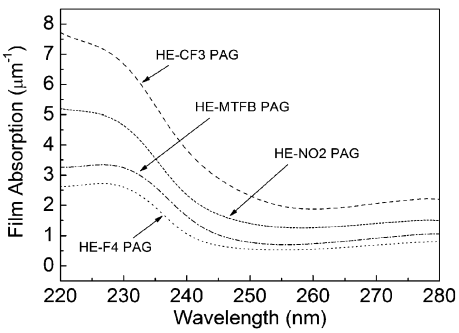

Fig. 3 DUV absorption of resist films.

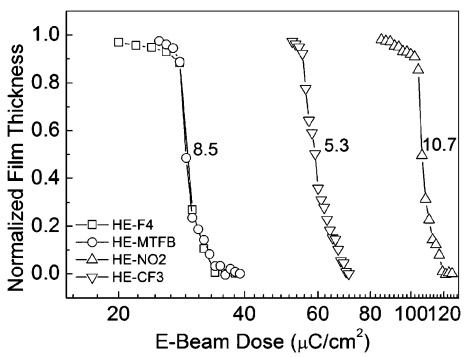

Fig. 4 Resist contrast curves under e-beam radiation.

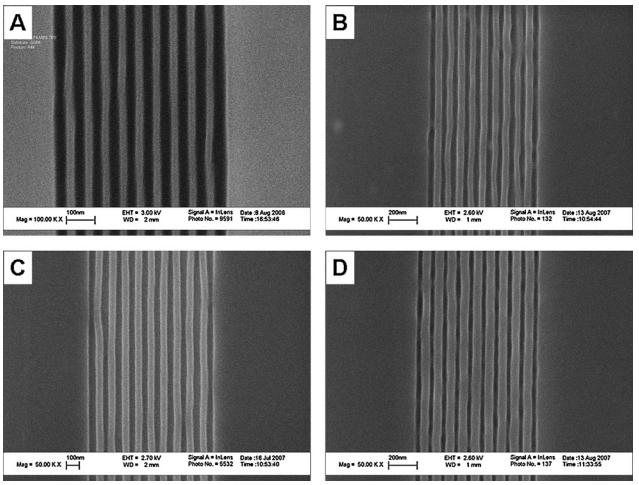

Fig. 5 SEM images of polymer-bound PAG resists pattern by 100 kV e-beam lithography and silicon nitride membrane. (A) HE-F4 PAG showed a 30 nm 1 : 1 line/space pattern. (B) HE-MTFB PAG showed a 40 nm 1 : 1 line/space pattern. (C) HE-NO2 PAG showed a 50 nm 1 : 1 line/space pattern. (D) HE-CF3 PAG showed a 45 nm 1 : 1 line/space pattern.

under electron-beam lithography are shown in Fig. 5. All resists used in this work were able to demonstrate 1 : 1 line/space resolutions at or below 50 nm using 100 keV e-beam exposure. The incorporation of the PAG anion into the polymer main chain confines the mobility of the photoacid generated in the resist film after exposure, which leads to reduced image blur and line slimming. This is not normally observed in chemically amplified resists without base quencher additives, due to photoacid diffusion during post-exposure bake (PEB) processing. The LER (3σ) measured on the 50 nm 1 : 1 line/space resist patterns of the HE-F4 PAG, HE-MTFB PAG, and HE-NO2 PAG resists were 3.20, 4.20, and 4.70 nm, respectively. The major limitation to finer imaging of these resist materials was observed to be pattern collapse during development and drying of the resist features. The HE-F4 PAG resist was found to produce the highest aspect ratio (2.3) features without pattern collapse while the other resists began to exhibit pattern collapse at aspect ratios greater than approximately 1.6. Based on the e-beam lithography performances, fluorinated PAG bound polymer resists were further initially investigated under EUV interference lithography: 40 nm, 32.5 nm (1 : 1) line/space patterns for HE-MTFB PAG and HE-F4 PAG resists were obtained at the dose of 18.8, 37.8 mJ cm^{-2}, respectively (see Fig. 6).

Atomic force microscopy (Veeco-NanoScope IV, Multimode AFM) provided 3-D topographic images of the lithographic patterns. The 3D rendering of 45 nm line space for HE-MTFB is represented in Fig. 7, which shows a smoother surface and a clearly defined sidewall. The depth profile analysis shows 15 to 20 nm vertical distances in the pattern. In order to be more accurate in the depth profile measurement, a high aspect ratio (HAR) tips purchased from Veeco were used in tapping mode for all the experiments. However it was noticed that in some cases, use of such tips could cause a damage of the lithographic pattern, typically along the scan direction. One of such, can be seen in the lower part of the image presented. In order to minimize pattern damage, all images were recorded at very low scan rate, regularly lower than 1 Hz. A study of the possible influence of tips with

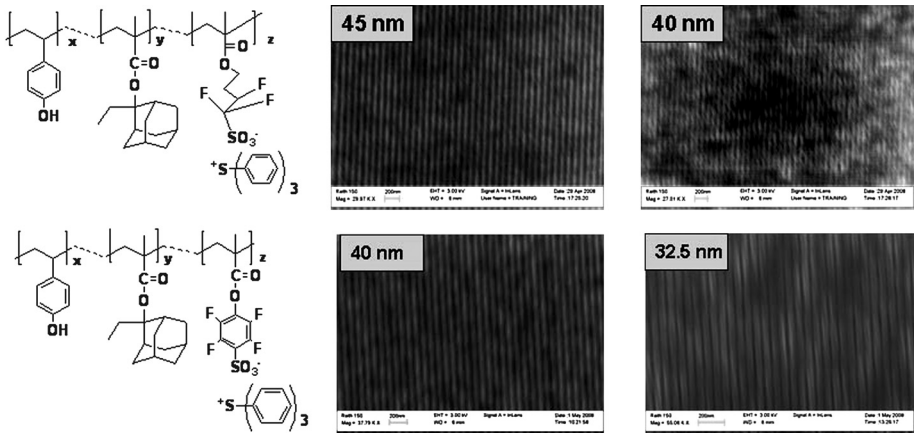

Fig. 6 SEM images of HE-MTFB PAG and HE-F4 PAG resist pattern (1 : 1 line/space) exposed under EUV interference lithography.

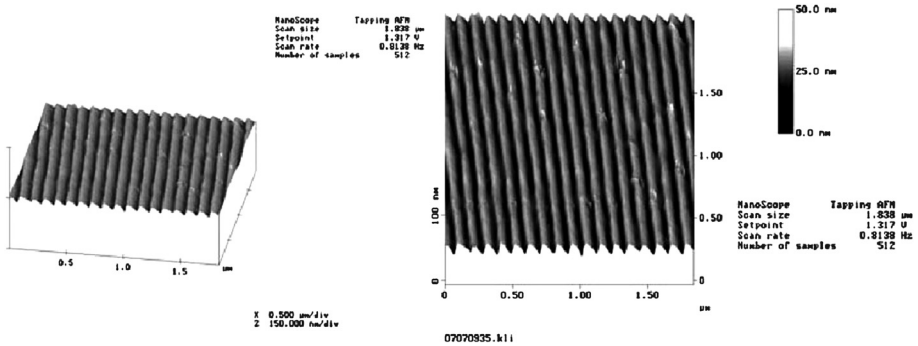

Fig. 7 AFM image of HE-MTFB PAG (45 nm line space features).

different aspect ratio, on the pattern shape and the appearance in AFM images is in progress.

4. Conclusion

A new series of anionic PAG bound polymeric resist based on hydroxystyrene and ethyl adamantly methacrylate comonomers were prepared and characterized. The goal of the work was to identify promising new PAG structures that could be incorporated into polymer-bound PAG resist designs for EUV lithography applications. Acid generation and absorption studies at DUV suggest that the new MTFB PAG and the previously reported F4 PAG are the most promising PAG monomers for EUV resist material design. Further investigation of the high resolution e-beam and initial EUV imaging performance demonstrated that the fluorinated PAG bound polymer resists, specially the MTFB PAG bound polymer resist are promising candidate CARs for EUV lithography, given further microstructure optimization. Further optimization of polymerization conditions, including kinetics of monomer incorporation and reactivity ratios will be reported subsequently.

Acknowledgements

The authors gratefully acknowledge Intel Corp. for financial support. Thanks to Ms M. Rabinovich for GPC analysis as well as Dr N. Pujari for SEM inspection.

References

1 *International Technology Roadmap for Semiconductors (ITRS)*, 2005, Lithography, http://public.itrs.net/.
2 B. Wu and A. Kumar, *J. Vac. Sci. Technol., B*, 2007, **25**(6), 1743.
3 R. H. Stulen and D. W. Sweeney, Extreme ultraviolet lithography, *IEEE J. Quantum Electron.*, 1999, **35**(5), 694.
4 J. M. J. Frechet, *Pure Appl. Chem.*, 1992, **64**, 1239.
5 M. Shirai and M. Tsunooka, *Bull. Chem. Soc. Jpn.*, 1998, **71**, 2483.
6 K. L. Covert and D. J. Russell, *J. Appl. Polym. Sci.*, 1993, **49**, 657.
7 H. Ito, *Adv. Polym. Sci.*, 2005, **172**, 37.
8 Y. Suzuki and D. W. Johnson, *Proc. SPIE*, 1998, **3333**, 735.
9 R. Ayothi, Y. Yi, H. Cao, W. Yueh, S. Putna and C. K. Ober, *Chem. Mater.*, 2007, **19**, 1434.
10 H. Mori, E. Nomura, A. Hosoda, Y. Miyake and H. Taniguchi, *Macromol. Rapid Commun.*, 2006, **27**, 1792.
11 J.-B. Kim, H.-J. Yun and Y.-G. Kwon, *Chem. Lett.*, 2002, 1064.
12 Y.-G. Kwon, J.-B. Kim, T. Fujigaya, Y. Shibasaki and M. Ueda, *J. Mater. Chem.*, 2002, **12**, 53.
13 T. Fujigaya, Y. Shibasaki and M. Ueda, *J. Photopolym. Sci. Technol.*, 2001, **14**, 275.
14 C. David, A. R. Tully and J. M. J. Frechet, *Adv. Mater.*, 2000, **12**, 1118.
15 H. Kudo, R. Hayashi, K. Mitani, T. Yokozawa, N. C. Kasuga and T. Nishikubo, *Angew. Chem., Int. Ed.*, 2006, **45**, 7948.
16 X. André, J. Lee, A. DeSilva, C. K. Ober, H. B. Cao, H. Deng, H. Kudo, D. Watanabe and T. Nishikubo, *Proc. SPIE-Int. Soc. Opt. Eng.*, 2007, **6519**, 65194B.
17 H. Shiono, H. Hada, H. Yukawa and H. Oizumi, *Proc. SPIE-Int. Soc. Opt. Eng.*, 2007, **6519**, 5193U.
18 M. D. Stewart, H. V. Tran, G. M. Schmid, T. B. Stachowiak, D. J. Becker and C. G. Willson, *J. Vac. Sci. Technol., B*, 2002, **20**, 2946.

19 N. N. Matsuzawa, H. Oizumi, S. Mori, S. Irie, E. Yano, S. Okazaki and A. Ishitani, *Microelectron. Eng.*, 2000, **53**, 671.
20 M.-X. Wang, N. D. Jarnagin, C.-T. Lee, C. L. Henderson, W. Yueh, J. M. Roberts and K. E. Gonsalves, *J. Mater. Chem.*, 2006, **16**, 3701.
21 M.-X. Wang, K. E. Gonsalves, W. Yueh and J. M. Roberts, *Macromol. Rapid Commun.*, 2006, **27**, 1590.
22 H. Wu and K. E. Gonsalves, *Adv. Mater.*, 2001, **13**, 195.
23 M. Thiyagarajan, K. Dean and K. E. Gonsalves, *J. Photopolym. Sci. Technol.*, 2005, **18**, 737.
24 T. Watanabe, Y. Fukushima, H. Shiotani, M. Hayakawa, S. Ogi, Y. Endo, T. Yamanaka, S. Yusa and H. Kinoshita, *J. Photopolym. Sci. Technol.*, 2006, **19**, 521.
25 M.-X. Wang, K. E. Gonsalves, M. Rabinovich, W. Yueh and J. M. Roberts, *J. Mater. Chem.*, 2007, **17**, 1699.
26 C.-T. Lee, M.-X. Wang, N. D. Jarnagin, K. E. Gonsalves, J. M. Roberts, W. Yueh and C. L. Henderson, *Proc. SPIE-Int. Soc. Opt. Eng.*, 2007, **6519**, 65191E.
27 C.-T. Lee, C. L. Henderson, M.-X. Wang, K. E. Gonsalves and W. Yueh, *J. Vac. Sci. Technol., B*, 2007, **25**, 2136.
28 J. W. Thackeray, M. D. Denison, T. H. Fedynyshyn, D. Kang and R. Sinta, *ACS Symp. Ser.*, 1995, **614**, 110.
29 M.-X. Wang, W. Yueh and K. E. Gonsalves, *Macromolecules*, 2007, **40**, 8220.
30 D. Pasini, J. M. Klopp and J. M. J. Frechet, *Chem. Mater.*, 2001, **13**, 4136.

